



CHORUS

This is the accepted manuscript made available via CHORUS. The article has been published as:

High-pressure dynamics of hydrated protein in bioprotective trehalose environment

S. O. Diallo, Q. Zhang, H. O'Neill, and E. Mamontov

Phys. Rev. E **90**, 042725 — Published 30 October 2014

DOI: [10.1103/PhysRevE.90.042725](https://doi.org/10.1103/PhysRevE.90.042725)

High pressure dynamics of hydrated protein in bio-protective trehalose environment

S.O. Diallo,^{1,*} Q. Zhang,² H. O'Neill,² and E. Mamontov³

¹*Quantum Condensed Matter Division, Oak Ridge National Laboratory, Oak Ridge, Tennessee 37831, USA*

²*Biology and Soft Matter Division, Oak Ridge National Laboratory, Oak Ridge, Tennessee 37831, USA*

³*Chemical and Engineering Science Division, Oak Ridge National Laboratory, Oak Ridge, Tennessee 37831, USA*

We present a pressure dependence study of the dynamics of lysozyme protein powder immersed in deuterated α,α -trehalose environment via quasi-elastic neutron scattering (QENS). The goal is to assess the baro-protective benefits of trehalose on bio-molecules by comparing the findings with those of a trehalose-free reference study. While the mean-square displacement of the trehalose-free protein (hydrated to $d_{D_2O} \simeq 40$ w%) as a whole, is reduced by increasing pressure, the actual observable relaxation dynamics in the pico-(ps) to nano-seconds (ns) time range remains largely unaffected by pressure - up to the maximum investigated pressure of 2.78(2) Kbar. Our observation is independent of whether or not the protein is mixed with the deuterated sugar. This suggests that the hydrated protein's conformational states at atmospheric pressure remain unaltered by hydrostatic pressures, below 2.78 Kbar. We also found the QENS response to be totally recoverable after ambient pressure conditions are restored. Small angle neutron diffraction measurements confirm that the protein-protein correlation remains undisturbed. We observe however a clear narrowing of the quasi-elastic neutron (QENS) response as the temperature is decreased from 290 K to 230 K in both cases, which we parametrize using the Kohlrausch-Williams-Watts (KWW) stretched exponential model. Only the fraction of protons that are immobile on the accessible time window of the instrument, referred to as the elastic incoherent structure factor (EISF) is observably sensitive to pressure, increasing only marginally but systematically with increasing pressure.

PACS numbers: 87.15.Vv, 28.20.Cz, 87.15.hm

I. INTRODUCTION

Understanding the mechanism by which organisms survive under extreme environments such as excessive heat and/or dehydration in arid or hot regions, unusual cold in the arctic, or elevated pressures at the bottom of the oceans, is a topic of chief scientific relevance in biology, and physiology [1–3]. While this survival ability has long been known to be due to the presence of non-reducing disaccharides, such as trehalose, in certain living cells and plants, the underlying process by which these sugars stabilize biological systems is far from being fully understood. Among its bio-protective benefits, trehalose is known for example to help preserve the structural integrity in halophiles and cyanobacteria [4], to serve as a carbon source or as a compatible solute for relieving high osmotic stresses in prokaryotes such as *Escherichia coli* during bio-synthesis [5]. For these reasons, trehalose is also commonly used in industry for preserving food, vaccines, and cosmetic products [3].

To date, two main scenarios have been proposed to explain how trehalose is able to serve as a good bio-protective agent, with some experimental evidence supporting both. Each proposal has only been able to explain a portion of the mechanism. Green and Angell [6] for example have related the resistance to extreme temperatures to the high glass transition temperature of trehalose with respect to that of pure water, which al-

lows for a protective vitrified sugar shield around bio-molecules. Crowe and collaborators [4], on the other hand, associated the resistance to drought to the ability of trehalose to establish strong hydrogen-bond-based interactions with the polar groups of bio-systems. In this latter scenario, trehalose is able to ‘replace’ water near biological surfaces, thereby preserving the hydrogen bond network even in the absence of water. The neutron diffraction measurements of Branca *et al.* [7, 8] reveal a strong distortion of the peaks linked to the hydrogen bonded network in the partial radial distribution functions for all disaccharides, and for trehalose in particular, consistent with this *replacement* theory. Various spectroscopy techniques [9–16] and molecular dynamics simulations [17–20] have consistently confirmed the slowing down of water molecules that are immersed in a trehalose environment at normal atmospheric pressure. This reduction in mobility is hypothesized to be linked to the formation of a more crystalline structure (a glassy shell that protects biological cells) as a result of hydrogen binding between the water and the trehalose molecules, consistent with Green and Angel’s *glassy shell* proposal [6]. While these represent important developments in the field, much work remains to be done before a full and complete picture can emerge regarding the mechanism by which trehalose facilitates bio-protection. An outstanding pertinent question in biology, is whether or not trehalose offers baro-protective benefits for bio-species and if so, to what extent and how.

Pressure is a clean thermodynamic tuning variable that can be used to define conformational states in protein [21, 22]. By varying pressure, it is possible to explore

*Electronic address: omardiallos@ornl.gov

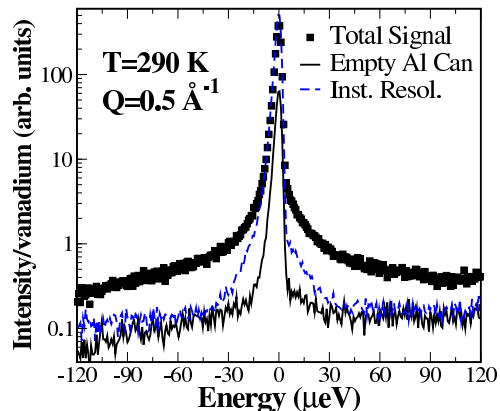


FIG. 1: Representative raw quasi-elastic neutron (QENS) response collected on the BASIS spectrometer at temperature $T = 290$ K and wavevector $Q = 0.5 \text{ \AA}^{-1}$. The black circles show the total signal from the D_2O -hydrated lysozyme powder in the Al container. The black solid line represents the signal from the empty high pressure Al cell and the blue dashed line shows the instrument resolution function, measured at 100 K using the same D_2O -hydrated sample.

the conformation space from the folded to the unfolded protein, as the partial molar volume is changed, and correlate these findings with the protein flexibility and various function. While the dynamics of hydration water around proteins and that of proteins [23–27] have been extensively investigated at ambient pressure, much less efforts have been devoted to high pressure research, owing primarily to technical limitations, which are now slowly being overcome.

A technique of choice for studying protein dynamics is Quasi-Elastic Neutron Scattering (QENS) because it provides direct and unique information on the internal diffusive modes of hydrogen atoms in protein and their spatial correlations, from which the global conformational fluctuations of the protein can be inferred [28–30]. Several studies of various globular protein and of trehalose-water compounds at ambient pressure have already been reported [9–11, 15, 31–33]. In a recent comprehensive study using both X-ray and neutrons, Ortore *et. al* [34] have simultaneously investigated the effect of high pressure on the structure and dynamics of lysozyme solution, up to about 1.5 Kbar. While they observe significant modifications in the protein-protein interaction potential just above 0.6 Kbar, they found no dramatic change in the protein globular structure with pressure. They found a strong correlation between the protein local dynamics and the water solvent, in agreement with an earlier QENS work on lysozyme in solution by Fillabozzi *et. al* [35] in which the pressure dependence of the dynamics of lysozyme in solution was examined up to ~ 1.2 Kbar.

We here present high precision QENS measurements

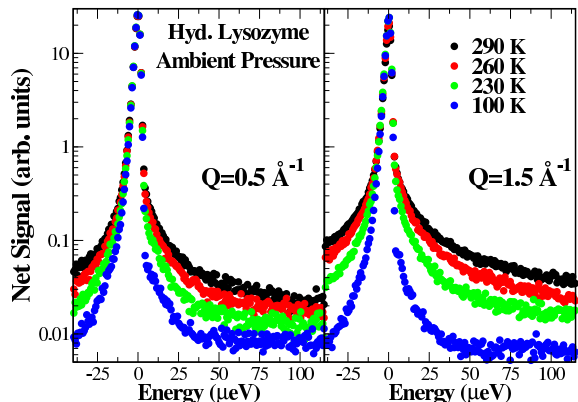


FIG. 2: Temperature dependence of the net QENS response from D_2O -hydrated lysozyme after subtraction of container contribution and vanadium normalization at $Q = 0.5 \text{ \AA}^{-1}$ (left panel) and $Q = 1.5 \text{ \AA}^{-1}$ (right panel). Data at 100 K was used as a reference resolution function to determine the characteristic relaxation parameters at the higher temperatures.

of D_2O -hydrated hen-egg-white lysozyme mixed with deuterated α, α -trehalose. Our aim is to evaluate how trehalose affects the dynamics of biological systems, when subjected to elevated pressures. Understanding how the dynamics of lysozyme respond to high pressure, below the protein denaturation pressure is an important goal of the present work. We find that beyond a slow but systematic decrease of the fraction of immobile hydrogens in the protein (methyl and non-methyls groups static on the accessible time window on the neutron instrument) with pressure, there is no significant impact on the characteristic relaxation times in the nano- to pico-seconds range at all temperatures investigated, up to 2.78 Kbar. Interestingly, we find the QENS response and characteristic relaxations to be recoverable after ambient conditions are restored. These results indicate that the slow dynamics of hydrated lysozyme do not change with increasing hydrostatic pressures, in agreement with previous QENS reports [34, 35] and MD simulations [36].

This article is organized as follows: technical aspects; primarily sample information and neutron measurements are presented in Sec. II. Sec. III discusses the data and fitting methods, followed by Sec. IV where the main results are presented. A summary is then presented in Sec.V.

II. EXPERIMENTAL DETAILS

A. Sample Preparation

The lysozyme (L4919; 98% purity) and deuterated α, α -trehalose samples were purchased from Sigma Aldrich,

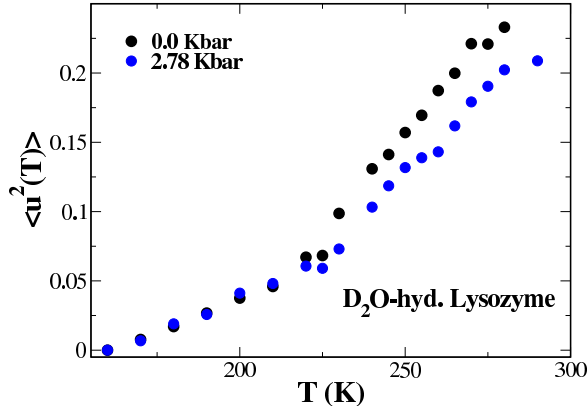


FIG. 3: Evolution of the mean square displacement (MSD) of hydrogens with motion faster than ~ 1 nanosecond, in D_2O -hydrated lysozyme powder with pressure. The harmonic behavior observed at low temperatures changes slope around 220 K. This anharmonicity at the high temperature goes down with increasing pressure. The data was calibrated with the reference MSD value $\langle u_0^2(T_0) \rangle$ at $T_0 = 150$ K.

and Omicron respectively. The labile hydrogen atoms in lysozyme were exchanged for deuterium by dissolving lysozyme in D_2O followed by lyophilization. This process was repeated 3 times to ensure complete exchange of the H atoms. The sample was then hydrated using isopiestic conditions by incubation in a sealed container containing respectively 99.9% of D_2O . The level of hydration was controlled by varying the incubation time. The hydration level was determined by the relative change in the sample weight following humidity exposure. The final hydration level was $d_{D_2O} \simeq 40\%$ of the original protein mass. In the case of the lysozyme-trehalose mixture, equal amounts of the protein and sugar were dissolved in D_2O followed by the lyophilization and hydration procedure described above. Approximately ~ 150 mg of powder was used to prepare each sample, and loaded into a specially designed high pressure Al cell.

B. Elastic and Quasi-Elastic Neutron Scattering

The neutron scattering measurements were performed on the backscattering spectrometer (BASIS) at the 1.4 MW Spallation Neutron Source, Oak Ridge National Laboratory (ORNL), USA [37], which has an energy resolution of $1.75 \mu\text{eV}$ (Half-Width at Half-Maximum) at the elastic line, and spans a wide range of momentum transfer and energy transfer, respectively $0.3 < Q < 1.9 \text{ \AA}^{-1}$, and $-120 < \omega < 120 \mu\text{eV}$. The useful QENS data were however analyzed over Q in the range $0.5 \leq Q \leq 1.5 \text{ \AA}^{-1}$. This was necessary to avoid coherent contribution from the protein at low and high Q 's. We used a helium gas

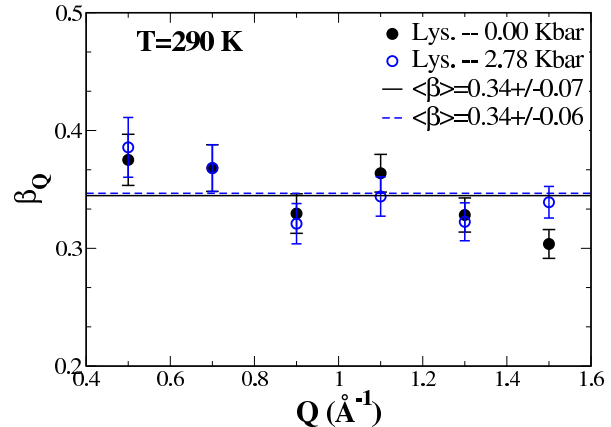


FIG. 4: Variation of the stretching exponent parameter β_Q with momentum transfer Q at temperature $T = 290$ K. Solid circles are the observed values at ambient pressure, and the open circles at $P = 2.78$ Kbar. The solid and dashed lines are the average values over all Q .

panel with an intensifier to increase the pressure inside a specially designed Al cell, sealing the cell for the rest of the experiment when the desired pressure is reached. This means that the high pressure measurements were all performed at constant volume (V_0), starting from 290 K and following the thermodynamic curve $P = [nRT/V_0]$ on cooling. Experiments were performed at ambient pressure (0.00), 1.00, 1.58, and 2.78 Kbar at three temperatures: 290 K, 260 K and 230 K for both samples. The instrument resolution function was measured using the ‘frozen’ sample at 100 K, where the proton mobility in the protein becomes resolution limited on the instrument. The empty can was also measured for data correction.

III. DATA ANALYSIS

Before any quantitative analysis, we first begin with a qualitative data inspection and simple comparison between the different spectra to look for trends and insure the observations are consistent with anticipated responses from the sample. We show as an example a representative raw spectra of hydrated lysozyme at $Q = 0.5 \text{ \AA}^{-1}$ and $T = 290$ K in Fig. 1. The instrument resolution function and the empty can data are also overlaid for comparison. The presented spectrum at each (P, T) point were collected on BASIS for approximately 3 hours when the SNS accelerator power was running at 1.2 MW. For the data presented, the corresponding temperature and pressure were stable within ± 0.5 K, and ± 20 bars, respectively. The contributions from the empty can to the QENS signal are largely limited to the elastic line and the linear background. We used a self-shielding factor of 1 to subtract the corresponding background. Fig.

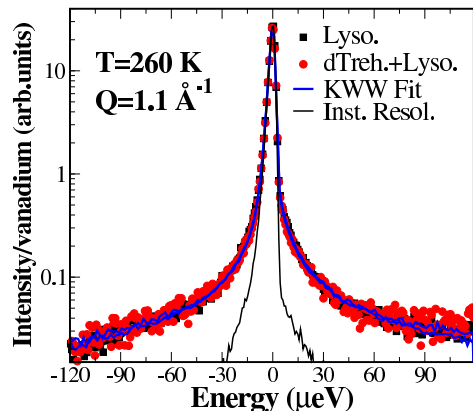


FIG. 5: Net observed signal (background subtracted) from the D₂O-hydrated protein compound without trehalose (black squares) and with trehalose (red circles). Solid black line shows the corresponding resolution function. The blue lines are the resulting fits to the data using a Kohlrausch-Williams-Watts (KWW) model, discussed in the text.

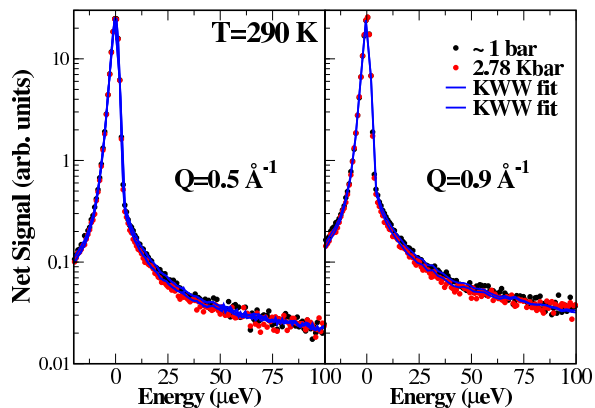


FIG. 6: Pressure dependence of the net response from D₂O-hydrated lysozyme at selected $Q=0.5 \text{ \AA}^{-1}$ (left panel) and $Q=0.9 \text{ \AA}^{-1}$ (right panel) at 290 K. Black circles are the data at ambient pressure (1 bar) and red circles at 2.78 Kbar. The blue lines are the fits to the data using a Kohlrausch-Williams-Watts (KWW) model, as discussed in the text.

2 shows the temperature dependence of the net signal of lysozyme at ambient pressure after proper background correction at some selected Q values. We observe a clear narrowing of the quasi-elastic neutron (QENS) response with decreasing temperature.

Just prior to and immediately after the long QENS measurements, we performed diagnostic ‘incoherent elastic intensity’ scans on the D₂O-hydrated lysozyme sample, free of any trehalose, to look for differences in the

global molecular fluctuations between 1 bar and 2.78 Kbar. The elastically scattered neutrons were recorded on heating from 150 K up to 290 K, in variable steps of 5 and 10 K, depending of the temperature range. The elastic intensity as a function of temperature was obtained by integrating the corresponding spectrum over a very small energy range comparable to that of the instrument resolution, for each Q . Assuming an isotropic flexibility in the motion of the hydrogens inside the protein, the mean square displacement $\langle u^2(T) \rangle$ (or MSD) can be calculated from the elastic intensity $I_s(T)$ using the expression $\langle u^2(T) \rangle = -\frac{3}{Q^2} \ln \left[\frac{I_s(T)}{I_s(T_0)} \right]$ where T_0 represent the lowest measured temperature of 150 K. Fig. 3 shows the derived MSD as a function of temperature for the two pressures investigated. The data was calibrated relative to the ambient pressure MSD $\langle u^2(T_0) \rangle$ at 150 K. As the temperature is increased, $\langle u^2(T) \rangle$ increases harmonically up to about 220-230 K where it starts to increase more rapidly with increasing temperature. This deviation from harmonic motions [38], commonly found in bio-molecules (e.g: proteins, DNA, RNA.), is generally referred to as the dynamical transition [25, 39–41]. From Fig. 3, it is clear that anharmonic effects at 2.78 Kbar are less prominent than those at ambient pressure, but they continue to be present. This departure from harmonic behavior is associated with the onset of molecular jumps between different sites at the high temperatures [42].

To analyze the QENS data, we fitted each spectra independently using the DAVE software package [43], according to the generic model $I(Q, \omega)$:

$$I(Q, \omega) = N(Q) \left[x(Q) \delta(\omega) + (1 - x(Q)) S_m(Q, \omega) \right] \otimes R(Q, \omega) + B(Q, \omega) \quad (1)$$

where $N(Q)$ is an arbitrary scale factor, $x(Q)$ represents the population fraction of immobile protons or the elastic incoherent structure factor (EISF), $\delta(\omega)$ is a delta function centered around zero energy transfer, $B(Q, \omega)$ is a residual background term in the form $B(Q, \omega) = B_1 + B_2(\omega + \omega_0)^{-1}$ (with ω_0 fixed to the elastic energy of 2080 μeV), $R(Q, \omega)$ is the resolution function, and $S_m(Q, \omega)$ is a model scattering function, which depends intrinsically on the sample. The internal dynamics of protein being far too complex to be represented by a ‘standard’ single Lorentzian function, we used a stretched exponential function, also referred to as Kohlrausch-Williams-Watts (KWW) model [44, 45] to fit the data:

$$S_m(Q, \omega) = \int_0^\infty dt e^{-[t/\tau(Q)]^{\beta_Q}} e^{i\omega t}. \quad (2)$$

Here $\tau(Q)$ represent the relaxation time at a particular Q , and β_Q the stretching exponent, typically found to be $0 < \beta_Q < 1$ for systems with glassy behavior such as proteins. This model makes physical sense and better accounts for the distribution in activation energy in the protein [41]. We note however that the present data alone provide

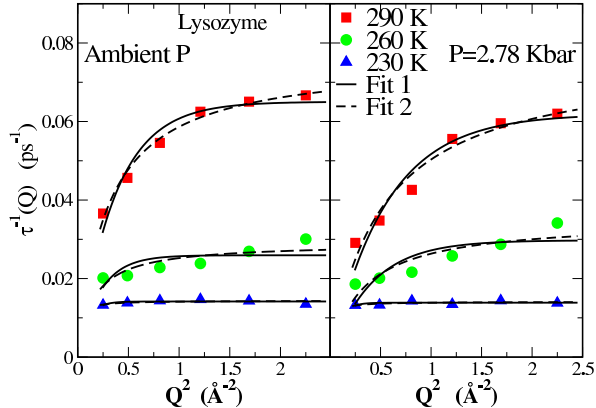


FIG. 7: Inverse τ_Q as a function of Q^2 for lysozyme at ambient pressure (left panel) and elevated pressure (right panel). Solid lines, denoted Fit 1, are fits of Eq. 3 to the observed values. Dashed lines (Fit 2) are fits of $\tau^{-1}(Q) = D_r Q^2 / (1 + D_r \tau_0 Q^2)$ to the data.

no clear evidence for either the ‘glassy or ‘replacement theories introduced earlier. Fig. 4 shows the variation of the observed stretching exponent β_Q of lysozyme with momentum transfer Q at $T = 290$ K. It is clear that β_Q has no significant dependence on Q , nor on pressure at 290 K, in agreement with previous work [31, 46]. We thus kept β_Q fixed to its average value of 0.34 in fitting the remainder of the data. This effectively reduces the free adjustable parameters to three: $N(Q)$, $x(Q)$ and $\tau(Q)$, excluding the background terms.

IV. RESULTS

A. Protein Response

Fig. 5 compares the ambient pressure QENS signal of lysozyme to that of the lysozyme-trehalose mixture at temperature $T = 260$ K and $Q = 1.1 \text{ \AA}^{-1}$. The lines represent the corresponding fits obtained with the KWW model. To the naked eye, there is no appreciable difference in the peak broadenings at this temperature. Further inspection of the data at other temperatures and pressures yield essentially the same results. We thus proceeded to capturing the temperature dependence of the peak broadening as a function of temperature for all pressure investigated, since thermal effects are much more important. Table I summarizes some of the key findings, which we discuss below.

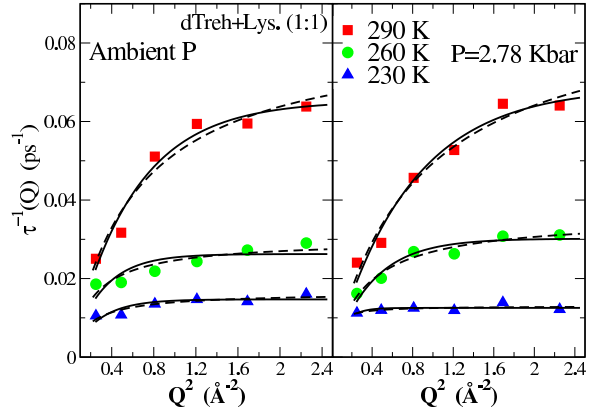


FIG. 8: Inverse τ_Q as a function of Q^2 for lysozyme and deuterated trehalose compound at selected pressures: ambient pressure (left panel) and elevated pressure (right panel). Labels are the same as in Fig. 7

B. Effects of Pressure

In this section, we evaluate how pressure affects the dynamics observed at atmospheric pressure. We begin first by investigating the trehalose-free sample with a comparative inspection of the ambient pressure data and that at 2.78 Kbar. Such a comparison is illustrated by Fig. 6, which shows the spectra collected at $T = 290$ K for two selected Q 's. For clarity, data at intermediate pressure values (1 and 1.58 Kbar) have been omitted but lie well within the two pressure limits. As can be seen, there is no observable change in the QENS lineshape, as pressure is increased slowly from 1 bar to 2.78 Kbar, suggesting that the relaxation dynamics on the pico- to nano-second scale are not perturbed by hydrostatic pressure, below 3 Kbar. We observe a very similar behavior with the data collected with the lysozyme immersed in trehalose. Nevertheless, we use Eqs. 1, and 2 to document the relaxation parameter $\tau(Q)$, and the $x(Q)$ at all temperatures and pressures probed. The variation of the inverse of the relaxation time $\tau(Q)$ with Q^2 is displayed in Figs. 7 and 8, for the two pressure limits: ambient and highest pressure. The relaxation dynamics at physiological temperature 290 K depicts the strongest dependence with Q , and suggests a jump diffusion behavior. This coupling with Q is reduced at 260 K, and barely noticeable at the lowest temperature of 230 K. To parametrize $\tau(Q)$, we use the following model [47]:

$$\frac{1}{\tau(Q)} = \frac{1}{\tau_r} (1 - e^{-D\tau_r Q^2}) \quad (3)$$

where τ_r is the residence time between jumps, and $D = \langle u^2 \rangle / 6\tau_r$ the self-diffusion coefficient, from which we compute the average diffusion coefficient $\langle D \rangle = D_r \times$

TABLE I: Temperature and pressure dependence of the characteristic parameters for the EISF, (p_s and p_f in Eq. 4), and of the average residence time $\langle\tau_{r_i}\rangle$, calculated using the expression $\langle\tau_{r_i}\rangle = \tau_{r_i}\Gamma(1/\beta_Q)/\beta_Q$. The τ_{r_i} were obtained from fits of Eq. 3 to the observed KWW $\tau(Q)$, i.e. $\tau(Q)^{-1} = \frac{1}{\tau_r}(1 - e^{-D\tau_r Q^2})$. The subscripts indicate the name of the sample, where $s=L$ is for lysozyme, and $s=LT$ indicates the lysozyme-trehalose compound.

T/K	P/Kbar	p_L	p_{LT}	f_L	f_{LT}	$\langle\tau_{r_L}\rangle/\text{ps}$	$\langle\tau_{r_{LT}}\rangle/\text{ps}$
290	0.00	0.489(1)	0.570(5)	0.820(1)	0.777(1)	85.3	85.3
	1.00	0.501(1)	0.550(1)	0.830(1)	0.789(2)	79.7	87.5
	1.58	0.510(1)	0.585(1)	0.841(1)	0.811(1)	88.6	101.5
	2.78	0.527(1)	0.570(1)	0.865(1)	0.809(1)	90.3	80.8
260	0.00	0.512(1)	0.590(1)	0.870(1)	0.880(1)	215.2	212.4
	1.00	0.601(1)	0.630(1)	0.890(1)	0.878(2)	216.9	195.7
	1.58	0.600(1)	0.630(1)	0.892(1)	0.880(1)	243.1	233.1
	2.78	0.630(1)	0.627(2)	0.890(1)	0.887(1)	187.3	185.1
230	0.00	0.740(1)	0.989(2)	0.939(1)	0.869(1)	393.6	379.1
	1.00	0.720(1)	0.877(1)	0.940(1)	0.930(1)	399.8	295.5
	1.58	0.731(1)	0.779(1)	0.940(2)	0.951(1)	413.7	384.7
	2.78	0.729(2)	0.801(4)	0.950(1)	0.940(1)	402.5	444.9

$\beta_Q/\Gamma(1/\beta_Q)$, where $\Gamma(x)$ is the Gamma function. The resulting fits are denoted ‘Fit 1’ in Fig. 7.

We found $\langle D \rangle$ to be more reliably determined at 290 K, with $\langle D \rangle$ in the range of $0.30\text{--}0.32 \times 10^{-5} \text{ cm}^2 \text{ s}^{-1}$ at ambient pressure and $0.16\text{--}0.18 \times 10^{-5} \text{ cm}^2 \text{ s}^{-1}$ at 2.78 Kbar in both samples. These values differ quantitatively from the $2.5\text{--}3 \times 10^{-5} \text{ cm}^2 \text{ s}^{-1}$ recently reported by Ortore *et al.* [34] for 10 weight % lysozyme in D_2O solution. This is not surprising since the determination of the average local diffusion coefficient is known to vary not just with the model used to extract it, but also on the protein concentration amount. At 260 K, $\langle D_r \rangle$ reduces down to $\sim 0.16\text{--}0.22 \times 10^{-5} \text{ cm}^2 \text{ s}^{-1}$ at zero pressure, and to $0.10\text{--}0.12 \times 10^{-5} \text{ cm}^2 \text{ s}^{-1}$ at the highest pressure. At 230 K however, the protein dynamics become observably so small that they fall within the instrument resolution. In this case, it becomes difficult to reliably resolve $\langle D_r \rangle$, as can be anticipated from the Q -behavior of $\tau(Q)$ shown by Figs. 7, and 8. The fitted $\langle D_r \rangle$ values at 230 K fluctuate nonetheless between $0.08\text{--}0.28 \times 10^{-5} \text{ cm}^2 \text{ s}^{-1}$ at all pressures investigated. We caution that this comparison holds only limited qualitative merits, given the significant difference in protein concentration between the solution used by Ortore *et al.* [34], and our powder samples. Our intent here is to put the present results in the context of recent work

To evaluate the influence of model on the diffusion coefficients, but also to improve the quality of the fits obtained for $\tau(Q)$, specially in light of the poorer fits at the high Q at 260 K, we have re-fitted the $\tau(Q)$ values using an alternative jump model $\tau^{-1}(Q) = D_r Q^2 / (1 + D_r \tau_0 Q^2)$. These fits are displayed as dashed lines and denoted ‘Fit 2’ in Figs. 7. With this alternate model, the observed diffusion coefficients at 290 K are indeed larger than those obtained with Eq. 3, yielding $\langle D_r \rangle \simeq 0.55 \times 10^{-5} \text{ cm}^2 \text{ s}^{-1}$ at ambient pressure which decreases to $0.25 \times 10^{-5} \text{ cm}^2 \text{ s}^{-1}$ at 2.78 Kbar. The corresponding values for the lysozyme+trehalose mixture are for instance $0.25 \times 10^{-5} \text{ cm}^2 \text{ s}^{-1}$ at ambient temperature and pressure

conditions, and $0.19 \times 10^{-5} \text{ cm}^2 \text{ s}^{-1}$ at the highest pressure. The $\langle\tau_0\rangle$ values obtained by this method are only marginally smaller than $\langle\tau_r\rangle$ of the KWW model introduced above, by about 2-5 ps. This offset does not impact the dependence of $\langle\tau_r\rangle$ on temperature or pressure. The average relaxation time $\langle\tau_{r_i}\rangle$ which accounts for the stretching effect of β_Q can also be computed using the expression, $\langle\tau_{r_i}\rangle = \frac{\tau_i}{\beta_Q} \Gamma(\frac{1}{\beta_Q})$, where τ_i equals to τ_r or τ_0 . The calculated $\langle\tau_{r_i}\rangle$ values using the fitted τ_r in Eq. 3 are reported in table I, along with other characteristic parameters. The subscript s in $\langle\tau_{r_i}\rangle$ indicates the name of the sample, where $s=L$ is for lysozyme, and $s=LT$ indicates the lysozyme-trehalose compound. Again, the strongest influence on this particular parameter is not pressure but rather temperature, to which we return below.

Based on the observations above, we concluded that the QENS broadening ($\tau(Q)$ parameter) is not a relevant parameter for evaluating the effects of pressure on protein or for assessing the baro-protection of trehalose, as we originally have hoped for. We instead focused our attention to the only observable quantity that shows some systematic and discernible change with pressure; the $x(Q)$ introduced in Eq. 1. This parameter yields valuable information on the geometry of active motions observed on the QENS instrument [23]. Fig.9 shows the $x(Q)$ parameter as a function of Q for several pressures for lysozyme at 290 K. While the behavior with Q appears to be the same, the magnitude of $x(Q)$ clearly increases with increasing pressure, suggesting that it is the population fraction - and not the relaxation times - of protons contributing to the different dynamical processes that gets affected by pressure. The dashed lines show fits to the data, based on the following coupled EISF model that accounts for contributions from both methyl groups and non-methyl groups:

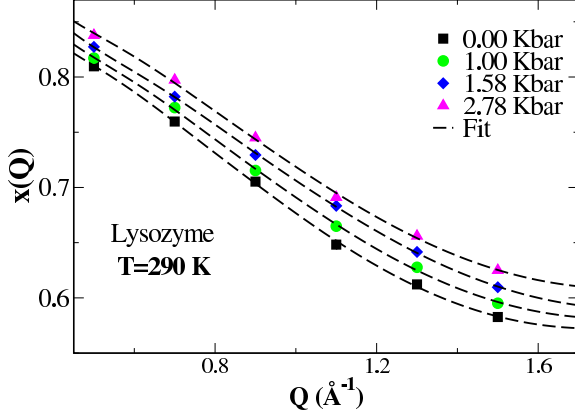


FIG. 9: Influence of pressure on the incoherent structure factor (EISF or $x(Q)$) of lysozyme at 290 K. Symbols represent results obtained respectively at ambient pressure (black squares), 1.00 Kbar (green circles), 1.58 Kbar (blue diamonds), and 2.78 Kbar (magenta triangles). Dashed lines are model fits to the data.

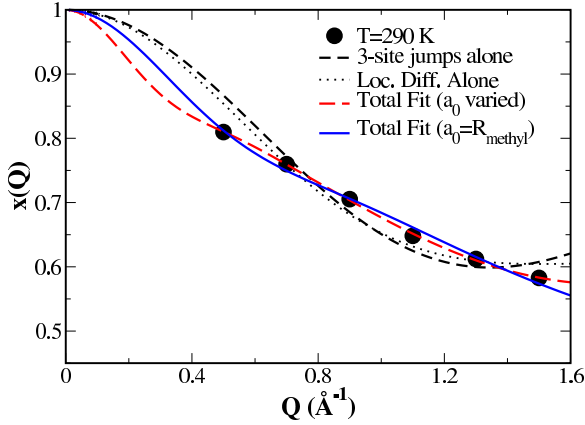


FIG. 10: Model fits to the elastic incoherent structure factor (EISF or $x(Q)$) of D_2O -hydrated protein at 290 K: black circles (experimental data); black short-dashed line (3-site jumps model); red long-dashed line (Eq. 4 with confining radius a_0 for methyls group allowed to vary); blue solid line (Eq. 4 with a_0 fixed to 1.1 Å, as observed previously [41]).

$$\begin{aligned}
 x(Q) &= x_{meth.}(Q) \times x_{loc.}(Q) \\
 &= \left[p_s + \frac{1-p_s}{3} \left(1 + 2j_0(Qa_0\sqrt{3}) \right) \right] \times \\
 &\quad \left[f_s + (1-f_s) \left(\frac{3j_1(Qa_1)}{Qa_1} \right)^2 \right]
 \end{aligned} \quad (4)$$

where p_s is the fraction of immobile observable protons

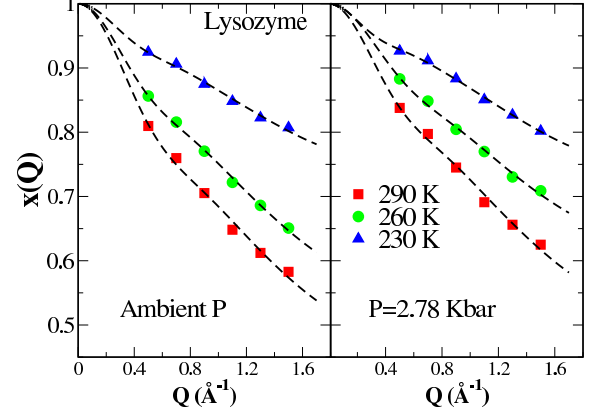


FIG. 11: Temperature dependence of the elastic incoherent structure factor (EISF or $x(Q)$) of lysozyme without trehalose: red squares (290 K), green circles (260 K), and blue triangles (230 K). The left panel shows the values at ambient pressure and the right panel indicates those at 2.78 Kbar. The dashed lines are fits of Eq. 4 with a_0 set to 1.1 Å.

associated with the methyl groups (3-fold jumps model), and f_s that associated with non-methyl groups (generic localized dynamics). Corresponding confining radii for both groups are represented by a_0 and a_1 , respectively. The model above was necessary in the absence of non-hydrated samples (dry) data that would have otherwise allowed us to characterize the methyl groups alone [46]. Fig. 10 illustrates the models used to fit the $x(Q)$ obtained at 290 K for lysozyme, with Eq. 4, and other variant fitting schemes. In fact, we used various models to fit a few selected $x(Q)$ before settling on that to use for the rest of the data. Specifically, we investigated a 3-sites jump model (assuming all contributions from methyl groups only), Eq. 4 with all parameters allowed to vary, and finally Eq. 4 with all but a_0 adjustable. In the later case, we set $a_0 = 1.1$ Å, its reported value in the literature [41]. Without this constraint, we get a somewhat larger a_0 , with $1.3 < a_0 < 1.7$ Å at all temperatures.

With the confining radii for methyl-groups fixed to its nominal value, fits to the $x(Q)$ shown in Figs. 11 and 12 yield an a_1 parameter in the range 3-5 Å at all temperatures for both samples. There is no clear systematic dependence of a_1 on pressure, within our limited Q -range. We observe a subtle pressure dependence of the population fraction contributing to the rotations of the methyl-groups and those that are not. These fractions p_s and f_s are all summarized in Table I. For a detailed account of the various contributing factors to the EISF in proteins, the reader is referred to Refs. [32, 41, 46].

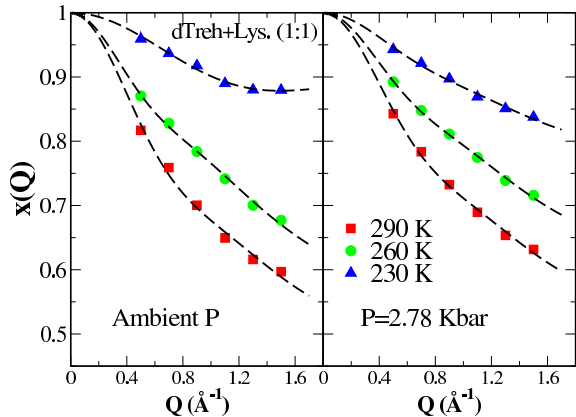


FIG. 12: Temperature dependence of the elastic incoherent structure factor (EISF or $x(Q)$) of lysozyme in deuterated trehalose environment.

C. Structure Conservation

Recent upgrades to the BASIS instrument offer high- Q resolution diffraction capability from about 0.15 to 1.9 \AA^{-1} . This added feature has allowed us to also investigate the low Q structure response (in the range 0.18-0.3 \AA^{-1}) during the dynamics measurements. The small angle neutron scattering data taken *in situ* reveal the existence of a structural peak which remains invariant with pressure, as shown by Fig. 13 for D_2O -hydrated protein. The peak revolves around 0.225 \AA^{-1} for both samples, and corresponds to protein-protein correlation length of about 28 \AA [48]. This monomer-monomer correlation peak appears to be marginally narrower in lysozyme-trehalose mixture (not shown) than in the bare lysozyme. It will be interesting to investigate the origin of this difference and to probe much larger length scales, which have been shown to be sensitive to modest pressures [34] with small angle scattering, and see what role if any trehalose plays in suppressing denaturation.

V. SUMMARY

The non-reducing disaccharide trehalose is widely known for its thermo-protective benefits for certain micro-organisms and plants in arid regions but its baro-protective properties have yet to be fully demonstrated. In the present study work, we have attempted to understand a consequence of the latter on the molecular dynamics of lysozyme protein which is submerged in trehalose. Although lysozyme does not unfold at the pressures investigated here, the dynamics may in fact be altered by pressures below the actual denaturation pressure. Understanding the effects of these non-denaturing pressures on the protein dynamics is thus important for

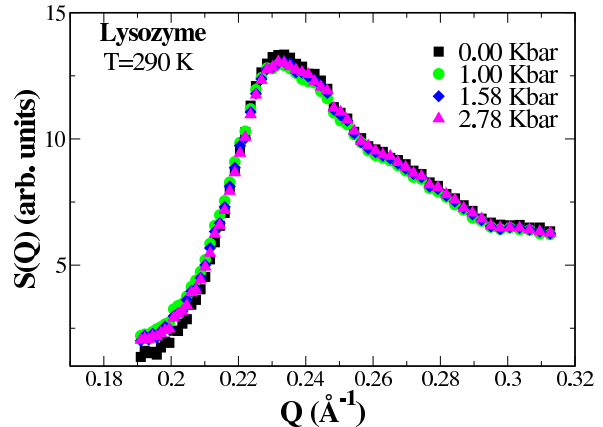


FIG. 13: Influence of pressure on the observed protein-protein peak in hydrated lysozyme at 290 K. Data were taken *in-situ* at BASIS using new diffraction detectors. Symbols represent results obtained respectively at ambient pressure (black squares), 1.00 Kbar (green circles), 1.58 Kbar (blue diamonds), and 2.78 Kbar (magenta triangles).

understanding the mechanism of pressure-driven unfolding. It is worthwhile noting here that structural studies of lysozyme in solution indicated it maintains its native, folded conformational state up to ~ 5 Kbar [49].

Our quasi-elastic neutron data indicates no significant slowing-down of the lysozyme dynamics as pressure is increased from ambient pressure to 2.78 Kbar independently of whether or not trehalose was present. The lack of any observable effect of pressure on the relaxation times of lysozyme indicates unambiguously that the overall secondary structure identity of the protein is indeed undisturbed by pressure, up to at least 2.78 Kbar. Because of this preservation of the structural integrity of the protein under the pressures probed in the present measurement, we are not able to elucidate the role played by trehalose in baro-protection of bio-molecules. One may be tempted to conclude that perhaps trehalose plays no baro-protection role since it has no particular impact on the QENS signal as pressure is varied, but such conclusion merits further investigation at the higher pressure where the protein actually unfolds and denatures.

In spite of this, we have been able to quantitatively document the evolution of the protein dynamics under hydrostatic pressure up to $\simeq 3$ Kbar, showing no significant changes in the relaxation times with pressure at any temperature. From model fits to the observed elastic incoherent structure factor ($x(Q)$), we have estimated the molecular fractions of hydrogens in lysozyme that are associated with relevant localized dynamics, as well as the corresponding spatial correlation lengths (3-5 \AA); differentiating between the contributions from the methyl groups, and those of other groups.

If indeed reversible protein unfolding occurs at medium

pressures via a solvent-mediated mechanism, as suggested by recent NMR studies [26], dynamical studies of different hydration-levels would be important to better understand baro-protection with trehalose. While this hypothesis can be excluded on the basis of the findings in Ref. [34] up to at least 1.5 Kbar, it has also been reported by Hedoux *et al.* [50] that the softening of the hydrogen bond network of water due to pressure, could subsequently induce a softer protein dynamics. The key point is that solvent-protein interactions are important, and that protein in solution, would respond differently to hydrostatic pressure than powders would. In fact, Refae *et al.* [26] argued using NMR data that buried water molecules play an important role in conformational fluctuation at normal pressures, and are implicated in the nucleation sites for structural changes leading to pressure denaturation or channel opening.

Future work could explore the effects of pressure on protein dynamics under increased hydration levels – but more importantly at the higher pressures, in excess of 6-7 Kbar, where Bridgman [51] first reported a denaturation of lysozyme. These pressures are unfortunately not currently achievable by our pressure intensifier, and are also limited by the design of our Al sample holder (rated to ~ 4.5 Kbar). While these represent major technical limitations, overcoming them will open up unprecedented

opportunities for conducting high pressure research in biological and chemical physics. Recent advances in high pressure cell design successfully tested in SANS measurements of lysozyme solution [52] could benefit future cell design for QENS measurements. In near-term experiments, it will be interesting to probe other proteins such as bacteriophage T_4 lysozyme for which unfolding has been observed [53] at pressures around ~ 2.5 Kbar.

Acknowledgments

We thank M. Rucker, S. Elorfi, and M. Loguillo for their excellent technical support with the high pressure equipments, and R. Goyette for his support at the beamline. Much gratitude is due to J. Carmichael for conceiving and designing the high pressure autofretage holder. We are grateful to W. Heller for critically reading the manuscript. HON and QZ acknowledge the support of the Center for Structural Molecular Biology at ORNL supported by the U.S. DOE, Office of Science, Office of Biological and Environmental Research Project ERKP291. Work at ORNL and SNS is sponsored by the Scientific User Facilities Division, Office of Basic Energy Sciences, US Department of Energy.

-
- [1] J. Clegg, *Comp. Biochem. Physiol., B: Comp. Biochem.* **128**, 613 (2001).
 - [2] E. P. Feofilova, *App. Biochem. Micro.* **39**, 1 (2003).
 - [3] A. Richards, S. Krakowka, L. Dexter, H. Schmid, A. Wolterbeek, D. Waalkens-Berendsen, A. Shigoyuki, and M. Kurimoto, *Food Chem. Toxicol.* **40**, 871 (2002).
 - [4] J. H. Crowe, L. M. Crowe, and D. Chapman, *Science* **223**, 701 (1984).
 - [5] J. C. Argüelles, *Archiv. of Microbiol.* **174**, 217 (2000).
 - [6] J. L. Green and C. A. Angell, *J. Phys. C: Solid State* **93**, 2880 (1989).
 - [7] C. Branca, S.V. Magazú, G. Maisano, F. Migliardo, and A.K. Soper, *Appl. Phys. A* **74**, s450 (2002).
 - [8] C. Branca, S.V. Magazú and F. Migliardo, *Rec. Res. Dev. Phys. Chem* **6**, 35 (2002).
 - [9] A. Faraone, S. Magazú, R. E. Lechner, S. Longeville, G. Maisano, D. Majolino, P. Migliardo, and U. Wanderlingh, *J. Chem. Phys.* **115**, 3281 (2001).
 - [10] I. Kóper, S. Combet, W. Petry, and M.-C. Bellissent-Funel, *Eur. Biophys. J.* **37**, 739 (2008).
 - [11] G. Lelong, D. L. Price, J. W. Brady, and M.-L. Saboungi, *J. Chem. Phys.* **127**, 065102 (2007).
 - [12] S. Magazú, V. Villari, P. Migliardo, G. Maisano, and M. T. F. Telling, *J. Phys. Chem. B* **105**, 1851 (2001).
 - [13] S. Magazú, F. Migliardo, and M. T. F. Telling, *J. Phys. Chem. B* **110**, 1020 (2006).
 - [14] S. Magazú, F. Migliardo, and A. J. Ramirez-Cuesta, *J. R. Soc. Interface* **4**, 167 (2007).
 - [15] F. Affouard, P. Bordat, M. Descamps, A. Lerbret, S. Magazú, F. Migliardo, A.J. RamirezCuesta and M.F.T. Telling, *Chem. Phys.* **317**, 258 (2005).
 - [16] G. S. Chryssomallis, P. M. Torgerson, H. G. Drickamer, and G. Weber, *Biochemistry* **20**, 3955 (1981).
 - [17] C. S. Pereira, R. D. Lins, I. Chandrasekhar, L. C. G. Freitas, and P. H. Hünenberger, *Biophys. J.* **86**, 2273 (2004).
 - [18] A. Lerbret, P. Bordat, F. Affouard, A. Hdoux, Y. Guinet, and M. Descamps, *J. Phys. Chem. B* **111**, 9410 (2007).
 - [19] S. Magazú, F. Migliardo, F. Affouard, M. Descamps, and M. T. F. Telling, *J. Chem. Phys.* **132** (2010).
 - [20] L. R. Winther, J. Qvist, and B. Halle, *J. Phys. Chem. B* **116**, 9196 (2012).
 - [21] W. Kauzmann, *Nature* **325**, 763 (1987).
 - [22] N. K. Jain and I. Roy, *Protein Science* **18**, 24 (2009).
 - [23] F. Gabel, *Eur. Biophys. J.* **34**, 1 (2005), ISSN 0175-7571.
 - [24] E. Mamontov, H. O'Neill, and Q. Zhang, *J. Biol. Phys* **36** (2010).
 - [25] W. Doster, *Eur. Biophys. J.* **37**, 591 (2008).
 - [26] M. Refae, T. Tezuka, K. Akasaka, and M. P. Williamson, *J. Mol. Biol.* **327**, 857 (2003).
 - [27] A. Benedetto, S. Magazú, F. Migliardo, C. Mondelli, and M. A. Gonzalez, *J. Phys. Conf. Ser.* **340**, 012093 (2012).
 - [28] J. M. Zanotti, M. C. Bellissent-Funel, and J. Parello, *Biophys. J.* **76**, 2390 (1999).
 - [29] G. Zaccai, *Science* **288**, 1604 (2000).
 - [30] F. Gabel, D. Bicout, U. Lehnert, M. Tehei, M. Weik, and G. Zaccai, *Quart. Rev. Biophys.* **35**, 327 (2002).
 - [31] M.-C. Bellissent-Funel, J.-M. Zanotti, and S. H. Chen, *Faraday Discuss.* **103**, 281 (1996).
 - [32] V. G. Sakai, S. Khodadadi, M. T. Cicerone, J. E. Curtis, A. P. Sokolov, and J. H. Roh, *Soft Mat.* **9**, 5336 (2013).
 - [33] S. Magazú, F. Migliardo, and A. Benedetto, *J. Phys.*

- Chem. B **114**, 9268 (2010).
- [34] M. G. Ortore, F. Spinozzi, P. Mariani, A. Paciaroni, L. R. S. Barbosa, H. Amenitsch, M. Steinhart, J. Olivier, and D. Russo, *J. R. Soc. Interface* **6**, S619 (2009).
- [35] A. Filabozzi, M. D. Bari, A. Deriu, A. D. Venere, C. Andreani, and N. Rosato, *J. Phys. Condens. Mat.* **17**, S3101 (2005).
- [36] V. Calandrini and G. R. Kneller, *J. Chem. Phys.* **128**, 065102 (2008).
- [37] E. Mamontov and K. Herwig, *Rev. Sci. Inst.* **82**, 085109 (2011).
- [38] T. Becker and J. C. Smith, *Phys. Rev. E* **67**, 021904 (2003).
- [39] S. H. Chen, L. Liu, E. Fratini, P. Baglioni, A. Faraone, and E. Mamontov, *Proc. Nat. Acad. Sci. U.S.A.* **103**, 9012 (2006).
- [40] L. Liu, A. Faraone, C.-Y. Mou, P.-C. Shih and S.-H. Chen, *J. Phys. Condens. Mat.* **16**, S5403 (2004).
- [41] J. Roh, J. Curtis, S. Azzam, V. Novikov, I. Peral, Z. Chowdhuri, R. Gregory, and A. Sokolov, *Biophys. J.* **91**, 2573 (2006).
- [42] W. Doster, S. Cusack, , and W. Petry, *Nature (London)* **337**, 754 (1989).
- [43] R.T. Azuah, L.R. Kneller, Y. Qiu, P.L.W. Tregenna-Piggott, C.M. Brown, J.R.D. Copley, and R.M. Dimeo,, *J. Res. Natl. Inst. Stan. Technol.* **114**, 341 (2009).
- [44] F. Mansour, R.M. Dimeo and H. Peemoeller, *Phys. Rev. E* **66**, 041307 (2002).
- [45] S. Takahara, N. Sumiyama, S. Kittaka, T. Yamaguchi, and M.-C. Bellissent-Funel, *J. Phys. Chem. B* **109**, 1123 (2005).
- [46] J. D. Nickels, V. Garcia-Sakai, and A. P. Sokolov, *J. Phys. Chem. B* **117**, 11548 (2013).
- [47] P.L. Hall and D.K. Ross, *Mol. Phys.* **42**, 673 (1981).
- [48] A. Stradner, H. Sedgwick, F. Cardinaux, W. C. K. Poon, S. U. Egelhaaf, and P. Schurtenberger, *Nature* **432**, 492 (2004).
- [49] M. A. Schroer, J. Markgraf, D. C. F. Wieland, C. J. Sahle, J. Möller, M. Paulus, M. Tolan, and R. Winter, *Phys. Rev. Lett.* **106**, 178102 (2011).
- [50] A. Hédoux, Y. Guinet, and L. Paccou, *J. Phys. Chem. B* **115**, 6740 (2011).
- [51] P. W. Bridgman, *J. Biol. Chem.* **19**, 511 (1914).
- [52] J. Kohlbrecher, A. Bollhalder, R. Vavrin, and G. Meier, *Rev. Sc. Inst.* **78**, 125101 (2007).
- [53] N. Nucci, B. Fuglestad, E. Athanasoula, and A. Wand, *Proc. Natl. Acad. Sci.* **111**, 13846 (2014).